

NoiseNCA: Noisy Seed Improves Spatio-Temporal Continuity of Neural Cellular Automata

Ehsan Pajouheshgar, Yitao Xu, Sabine Süsstrunk

School of Computer and Communication Sciences, EPFL, Switzerland
{ ehsan.pajouheshgar, yitao.xu, sabine.sustrunk }@epfl.ch

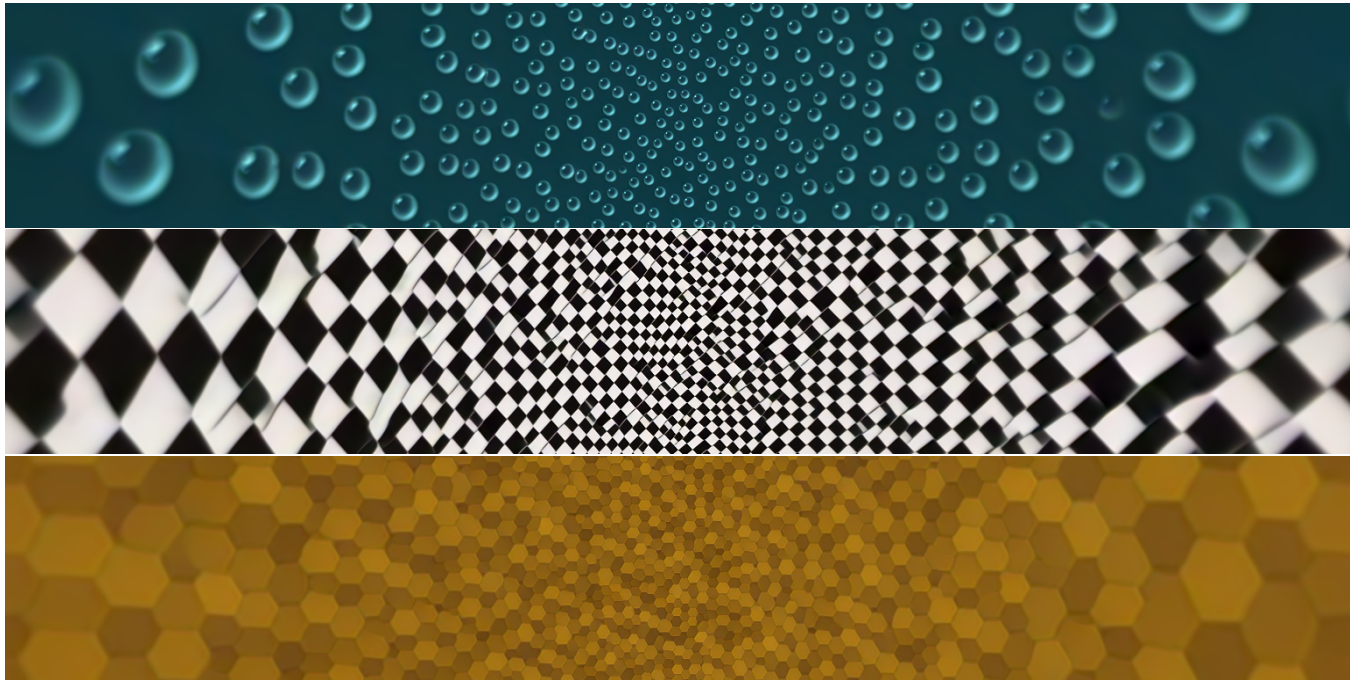


Figure 1: The update rule learned by *Noise-NCA* generalizes across different granularities of space and time discretization. This allows our model to synthesize textures at varying scales and speeds. Illustrated here, when changing the cell size across the space, *Noise-NCA* creates textures at varying scales within the same grid. For more results and an interactive demo, please check our webpage at <https://noisenca.github.io>

Abstract

Neural Cellular Automata (NCA) is a class of Cellular Automata where the update rule is parameterized by a neural network that can be trained using gradient descent. In this paper, we focus on NCA models used for texture synthesis, where the update rule is inspired by partial differential equations (PDEs) describing reaction-diffusion systems. To train the NCA model, the spatio-temporal domain is discretized, and Euler integration is used to numerically simulate the PDE. However, whether a trained NCA truly learns the continuous dynamic described by the corresponding PDE or merely overfits the discretization used in training remains an open question. We study NCA models at the limit where space-time discretization approaches continuity. We find that existing NCA models tend to overfit the training discretization, especially in the proximity of the initial condition, also called "seed". To address this, we propose a solution that utilizes

uniform noise as the initial condition. We demonstrate the effectiveness of our approach in preserving the consistency of NCA dynamics across a wide range of spatio-temporal granularities. Our improved NCA model enables two new test-time interactions by allowing continuous control over the speed of pattern formation and the scale of the synthesized patterns. We demonstrate this new NCA feature in our interactive online demo. Our work reveals that NCA models can learn continuous dynamics and opens new venues for NCA research from a dynamical systems' perspective.

Introduction

For decades, Cellular Automata (CA) have served as the foundation for studying and creating life-like systems (Von Neumann et al., 1966; Gardner, 1970), demonstrating how simple local interactions can lead to complex and emer-

gent behaviors (Wolfram and Gad-el Hak, 2003). Neural Cellular Automata (NCA) extend the classical CA framework by employing a neural network to define the update rule. This neural network can be trained using gradient descent, allowing NCA to learn complex dynamics from data. This has led to promising applications in texture synthesis (Niklasson et al., 2021b; Pajouheshgar et al., 2023a,b), modeling morphogenesis (Mordvintsev et al., 2020), image generation (Palm et al., 2022; Otte et al., 2021; Tesfaldet et al., 2022), and discriminative tasks (Randazzo et al., 2020; Sandler et al., 2020).

NCA models operate on a discrete grid of cells, where each cell’s state evolves over time according to a local update rule. The NCA update rule is inspired by Partial Differential Equations (PDEs) that describe reaction-diffusion systems (Turing, 1990) and can be viewed as an Euler integration of the PDE over a discretization of space and time. A key question surrounding NCA is whether it can truly capture underlying continuous dynamics or simply overfits the discrete representations used during training. We investigate this question by studying NCA behavior across different spatio-temporal granularities and at the limit where space-time discretization approaches continuity. In this work, we focus on NCA models trained for texture synthesis.

We find that existing NCA models, depending on the target texture, can fail to generalize to spatio-temporal granularities different from the training discretization (Niklasson et al., 2021b; Pajouheshgar et al., 2023b). We hypothesize that the overfitting occurs due to NCA’s reliance on stochastic updates to break the initial symmetry between the cells. We propose a simple, yet effective solution to this problem by removing the stochastic updates from the NCA architecture and initializing the cell states with random uniform noise. We call this approach *Noise-NCA*.

Through qualitative and quantitative evaluations, we show that *Noise-NCA* significantly improves the consistency of NCA dynamics across different granularities of space and time discretization. Furthermore, our improved NCA model unlocks two new test-time interaction capabilities: continuous control over the speed of pattern formation and the scale of the synthesized textures. We demonstrate these functionalities in an online demo available at <https://noisenca.github.io>. Our work reveals NCAs’ ability to learn continuous dynamics, opening new avenues for exploring them from a dynamical systems’ perspective.

Related Works

Neural Cellular Automata

Inspired by Alan Turing’s seminal work on Reaction-Diffusion (RD) systems (Turing, 1990), Mordvintsev et al. (2020) propose Neural Cellular Automata (NCA) as a variant of RD systems. Unlike traditional RD systems that require manual design and parameter tuning to create a desired pattern, NCA models can be trained using gradient de-

scent. The authors draw a parallel between NCA and dynamical systems to motivate their design choices. Niklasson et al. (2021b) further strengthen this relationship by formalizing the NCA training as numerically solving a Partial Differential Equation (PDE) defined on the cell states. NCA models have been successfully applied in various domains (Pajouheshgar et al., 2023a,b; Mordvintsev and Niklasson, 2021; Palm et al., 2022; Tesfaldet et al., 2022; Randazzo et al., 2020; Sandler et al., 2020). Despite these advances, most studies employing NCA have merely treated the model as a numerical method for solving the underlying dynamics, with barely any attention paid to whether NCA captures continuous dynamics or overfits discrete representations.

NCA as Partial Differential Equations

Mordvintsev et al. (2021) first investigate whether the spatio-temporal discretization used to train their differentiable RD system can effectively approximate a continuous PDE. However, their model lacks a directional spatial gradient and only involves local isotropic information. This sets them apart from common NCA models (Mordvintsev et al., 2020; Niklasson et al., 2021b; Pajouheshgar et al., 2023a,b) where cells perceive their neighborhood in a direction-sensitive manner. Moreover, they do not provide a solution for the cases where the model diverges from the expected behavior under the governing PDE. Niklasson et al. (2021a) explore the Growing NCA model (Mordvintsev et al., 2020) from the perspective of asynchronicity in the update rule and find that a globally synchronous update scheme negatively impacts the temporal continuity of NCA. However, the range of temporal discretizations examined in their work is very limited, leaving the behavior of NCA at the continuous-time limit as an open question. Furthermore, their findings indicate that NCA models, even with asynchronous updates, are prone to overfitting the training discretization. We extend upon previous analyses by pushing NCA to the continuous space-time limit and introduce a simple yet effective solution to improve the spatio-temporal continuity of NCA models.

Method

Neural Cellular Automata (NCA) models are a type of Cellular Automata models distinguished by the special characteristic that their update rules are governed by neural networks. In the following sections, we review NCA and introduce the notation that will be used later. In this article, we focus on 2D NCA models; nevertheless, a similar analysis to ours can be performed on other variants of NCA models.

Definitions

NCA models operate on a group of cells arranged in a 2D grid. These cells change over discrete time steps according to the NCA update rule. Let $S(x, y, t) \in \mathbb{R}^C$ denote the C dimensional vector that describes the state of a cell at loca-

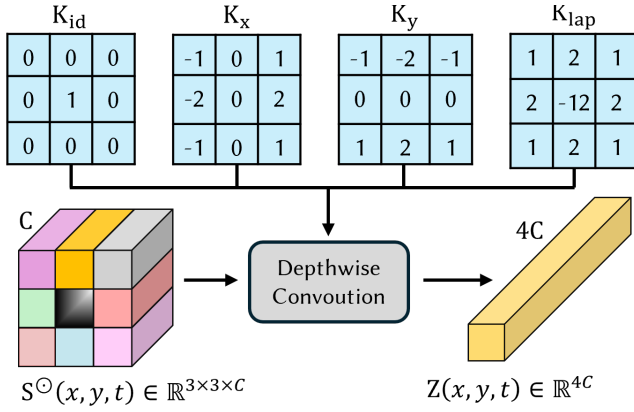


Figure 2: Overview of the *perception* stage in NCA models for a single cell. Depthwise convolution with the shown filters results in a 4x expansion of the number of channels in the perception vector Z .

tion (x, y) at time t . Note that

$$(x, y) \in \{0, 1, \dots, H-1\} \times \{0, 1, \dots, W-1\}$$

where H, W are the height and width of the grid, respectively. We define $S^\circ(x, y, t)$ as a set that contains the state of all cells in the neighborhood of a given cell¹. The most common neighborhood used in NCA models is the 9-point Moore neighborhood.

NCA Update Rule

As in any Cellular Automata, the NCA update rule is *local* and *space/time invariant*. Locality implies that, at each update step, a cell can only be influenced by a limited number of cells, namely its neighboring cells. Space-Time invariance means that all cells follow the same update rule, which does not change over time. Pajouheshgar et al. (2023a) suggested that the NCA update rule can be decomposed into *perception* and *adaptation* stages.

Perception Stage In this stage, each cell gathers information from its neighborhood to form its perception vector $Z(x, y, t)$ by applying depth-wise convolution on the state of cells in its neighborhood $S^\circ(x, y, t)$:

$$Z(x, y, t) = [K_{id}, K_x, K_y, K_{lap}] * S^\circ(x, y, t) \quad (1)$$

where $K_{id}, K_x, K_y, K_{lap}$ denote Identity, Sobel-X, Sobel-Y, and Laplacian filters. Note that the perception stage is non-parametric and convolution filters are frozen during training. These filters can be modified in test time to interactively control the behavior of cells (Niklasson et al., 2021b; Pajouheshgar et al., 2023a,b).

Adaptation Stage In the adaptation stage, cells can only rely on their perception vector and do not have access to

¹Note that the neighborhood can also contain the cell itself.

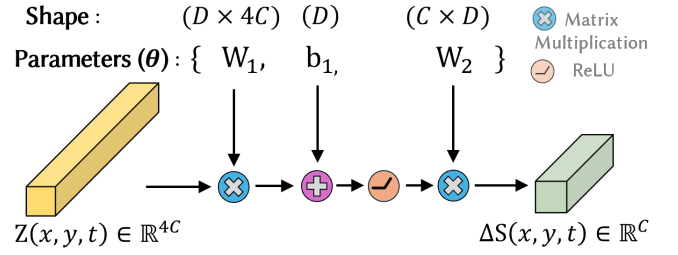


Figure 3: Overview of the *adaptation* stage in NCA models for a single cell. The perception vector goes through a series of operations to compute the residual cell update. C and D denote the number of channels in the cell state and the dimensionality of hidden layer, respectively.

the state of their neighbors. The perception vector passes through a neural network with two layers and a ReLU non-linearity, as shown in Figure 3. NCA parameters (θ) include the weights and bias of the first linear layer W_1, b_1 , and the weights of the second linear layer W_2 . The output of the adaptation stage is the residual update for each cell:

$$\Delta S(x, y, t) = W_2 (W_1 Z(x, y, t) + b_1)_+ \quad (2)$$

where $(\cdot)_+$ denotes the ReLU non-linearity. The final equation describing the cell update can be written as

$$S(x, y, t + \Delta t) = S(x, y, t) + \Delta S(x, y, t) \delta(x, y, t) \Delta t \quad (3)$$

where $\delta(x, y, t) \sim \text{Bernoulli}(\frac{1}{2})$ is a binary random variable. Multiplying the residual updates by δ breaks the symmetry between the cells and allows creating new textures over time by introducing randomness into the updates.

Training Scheme

We use the same training strategy to train all three NCA variants: *Vanilla-NCA*, *PE-NCA*, and our *Noise-NCA*. To train the model, we start from an initial state $S(x, y, t = 0)$ and iteratively apply the NCA update rule to obtain the cell states $S(x, y, t)$ at time t . The RGB image is then extracted by taking the first 3 channels of $S(x, y, t)$ and compared to the target texture using a loss function. We use the appearance loss function proposed by Pajouheshgar et al. (2023b) which measures the similarity of two texture images using a pre-trained VGG16 network (Simonyan and Zisserman, 2015). The gradients from the loss function are backpropagated through time and used to optimize the NCA parameters (θ) . The models are trained at resolution of $H, W = (128, 128)$. We use the pool technique proposed by Mordvintsev et al. (2020) to improve the long-term stability of the update rule.

Update Rule As a PDE

The NCA update rule in Equation 3 can be viewed as an Euler integration over a **spatio-temporal discretization of**

a **continuous PDE**² of the following form:

$$\frac{\partial S}{\partial t} = f_{\theta}(S, \nabla_x S, \nabla_y S, \nabla^2 S) \quad (4)$$

In the *Perception* stage, the spatial derivatives including ∇_x , ∇_y , and ∇^2 are estimated using Sobel filters K_x , K_y and 9-point discrete Laplacian kernel K_{lap} , respectively. In the *Adaptation* stage, the cell states are updated using Euler integration with timestep Δt . Note that the Sobel and Laplacian filters used in the *Perception* stage need to be divided by the cell size Δx , Δy to get consistent estimations of the spatial derivatives across different resolutions. From the finite difference perspective, a consistent approximation of spatial gradients using Sobel filters can be achieved using:

$$\nabla_x, \nabla_y \approx \frac{K_x}{\Delta x}, \frac{K_y}{\Delta y}$$

For the Laplacian operator, we first need to decompose it into second-order derivatives with respect to x , y , which can be written as $\nabla^2 = \frac{\partial^2}{\partial x^2} + \frac{\partial^2}{\partial y^2}$. Similarly, the Laplacian convolution kernel can be decomposed to two terms:

$$K_{\text{lap}} = K_{\text{lap}}^x + K_{\text{lap}}^y$$

$$\begin{bmatrix} 1 & 2 & 1 \\ 2 & -12 & 2 \\ 1 & 2 & 1 \end{bmatrix} = \begin{bmatrix} 0.5 & 0 & 0.5 \\ 2 & -6 & 2 \\ 0.5 & 0 & 0.5 \end{bmatrix} + \begin{bmatrix} 0.5 & 2 & 0.5 \\ 0 & -6 & 0 \\ 0.5 & 2 & 0.5 \end{bmatrix}$$

Therefore a discretization-consistent approximation of the Laplacian can be written as:

$$\nabla^2 \approx \frac{K_{\text{lap}}^x}{\Delta x^2} + \frac{K_{\text{lap}}^y}{\Delta y^2}$$

Combining the different pieces to make the NCA perception stage consistent across different spatial granularities, the convolution filters need to be modified as follows:

$$[K_{\text{id}}, K_x, K_y, K_{\text{lap}}] \rightarrow \left[K_{\text{id}}, \frac{K_x}{\Delta x}, \frac{K_y}{\Delta y}, \frac{K_{\text{lap}}^x}{\Delta x^2} + \frac{K_{\text{lap}}^y}{\Delta y^2} \right] \quad (5)$$

The cell size $(\Delta x, \Delta y)$ and timestep Δt are all set to 1.0 during training, but can be changed in test time to evaluate the NCA model across different spatial and temporal sampling granularities. Ideally, we want the learned NCA update rule to correspond to the PDE in Equation 4 and to be able to generalize to different Δt and $(\Delta x, \Delta y)$ in test time.

Baseline NCA models

We analyze and experiment with two NCA baselines. The first baseline is the model proposed by Niklasson et al. (2021b). Figures 2 and 3 accurately depict its architecture, which we refer to as *Vanilla-NCA*. The second baseline

²Technically a Stochastic Differential Equation (SDE) due to presence of $\delta(x, y, t)$ in the update rule.

is adapted from the DyNCA model by Pajouheshgar et al. (2023b). We refer to it as *PE-NCA* where PE is short for positional encoding. *PE-NCA* appends the normalized cell coordinates $(\frac{x}{H}, \frac{y}{W})$ to the perception vector $Z(x, y, t)$, which allows the cells to be aware of their position and thus making W_1 a $(D \times 4C + 2)$ matrix. Note that *Vanilla-NCA* uses circular padding when applying convolution kernels in the perception stage, while *PE-NCA* uses replicate padding to make the boundary condition consistent with positional encoding. In both of these baselines, the initial state³, is set to zero $S(x, y, t = 0) = 0.0$. The *Vanilla-NCA* model relies only on the stochastic update mask $\delta(x, y, t)$ to break the symmetry between cells in the initial state $t = 0$, while the positional encoding in *PE-NCA* acts as another source to differentiate between cells.

Proposed Model: NoiseNCA

We propose a simple yet effective change to the baseline NCAs that will prevent the model from overfitting to the training discretization. Our proposed NCA model, namely *Noise-NCA* is very similar to the *Vanilla-NCA* with the main difference being that we use random uniform noise as the initial state, i.e., seed

$$S(x, y, t = 0) \sim \mathcal{U}[-\epsilon, \epsilon] \quad (6)$$

where ϵ represents the strength of the noise. By setting the initial condition to random noise, *Noise-NCA* perfectly breaks the symmetry between cells and eliminates the need for stochastic update in the update rule. Therefore, *Noise-NCA*'s update rule is deterministic and can be written as :

$$S(x, y, t + \Delta t) = S(x, y, t) + \Delta S(x, y, t)\Delta t. \quad (7)$$

In the experiments section we evaluate all three NCA variants to see whether the learned update rule of each model corresponds to a continuous dynamic described by the PDE in Equation 4 or merely overfits to the training discretization. Our approach is to analyze the behavior of NCA models at the continuous limit where the temporal $\Delta t \rightarrow 0^+$ and spatial $\Delta x, \Delta y \rightarrow 0$ discretizations become more and more fine-grained. Our experiments demonstrate the advantages of *Noise-NCA* over the baselines through qualitative and quantitative evaluations.

Experiments

We train the three NCA variants - *Vanilla-NCA*, *PE-NCA*, *Noise-NCA* - on 45 different textures taken from Pajouheshgar et al. (2023b) using the training scheme described previously. We conduct qualitative and quantitative experiments to evaluate the trained NCA models at continuous-time limit $\Delta t \rightarrow 0^+$ and continuous-space limit $\Delta x, \Delta y \rightarrow 0$. In the paper, the qualitative results are demonstrated for two textures: "bubbly_0101", and "grid_0135".

³Also called seed

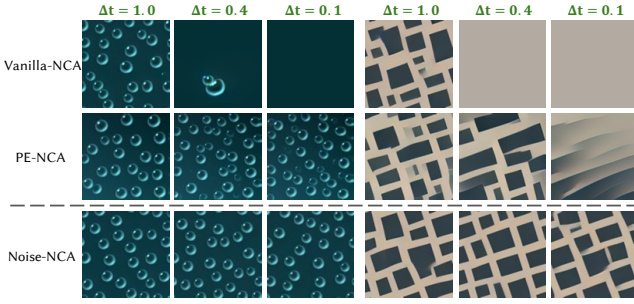


Figure 4: Output of NCA models for different values of Δt used in the Euler integration on two different textures. As Δt decreases, the patterns created by *Vanilla-NCA* and *PE-NCA* start to deviate from the correct pattern, while *Noise-NCA* is able to maintain the correct pattern across all values of Δt .

The complete qualitative results, which compare different NCA variants on all 45 textures, are available at <https://noisenca.github.io/supplementary/>. For a quantitative evaluation, we train and test the models on all of the 45 textures and use the appearance loss proposed by Pajouheshgar et al. (2023b) as a metric to quantify the quality of the NCA output for different values of Δt and $\Delta x, \Delta y$.

Continuous-Time Limit

Given a $\Delta t \leq 1.0$ and a simulation time T , we start from the initial state $S(x, y, t = 0)$ and use Euler integration to find $S(x, y, t = T)$ by applying the NCA update rule for $\lceil \frac{T}{\Delta t} \rceil$ steps. We set $T = 300$ in our experiments. Figure 4 shows the output of all three NCA variants on two different textures for $\Delta t \in \{1.0, 0.4, 0.1\}$. As shown in the figure, when $\Delta t = 1.0$ all models successfully create the correct patterns. However, as we decrease Δt the *Vanilla-NCA* and *PE-NCA* fail to synthesize the correct texture. On the contrary, *Noise-NCA* is able to successfully generate the correct pattern across all values of Δt .

For a more rigorous comparison, we perform a quantitative evaluation on 45 different textures for Δt values ranging from $[10^{-3}, 10^0]$. Let $S_T^{\Delta t}$ denote the output of NCA at time T when Δt is used as the integration timestep. For each value of Δt , we evaluate

$$\frac{\mathcal{L}(S_T^{1.0})}{\mathcal{L}(S_T^{\Delta t})}$$

where \mathcal{L} is our appearance loss function. This metric allows us to quantify, for each NCA variant, the relative output quality when the inference timestep Δt is different from the training timestep $\Delta t = 1.0$. The results in Figure 5 demonstrate that while the baseline NCAs fail to generalize to timesteps smaller than $\Delta t \leq 1.0$, *Noise-NCA* is able to maintain a consistent output quality even for very small values of Δt . This suggests that *Noise-NCA* is able to learn a continuous dynamic described by the PDE in Equation 4.

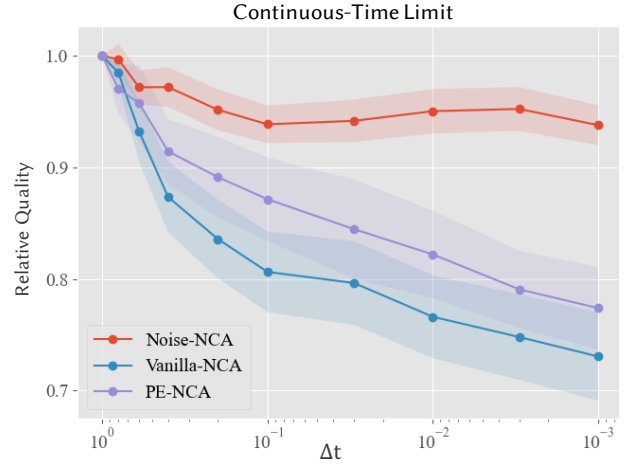


Figure 5: For each NCA variant, we evaluate the relative output quality for different values of Δt used for Euler integration and show the results averaged over 45 different textures. *Noise-NCA* shows significantly better generalization to different timesteps compared to the baseline NCAs, even for very small values of Δt .

Continuous-Space Limit

We evaluate the NCA models at the continuous-space limit by increasing the spatial resolution of the grid. In our experiments, we set $\Delta x = \Delta y$ for simplicity and use a square grid with size $H = W = \lceil \frac{128}{\Delta x} \rceil$, with 128×128 being the resolution used during training. To visualize and compare the results, we resize the NCA output from $H \times W$ to 128×128 . Notice that, as shown in Equation 5, for $\Delta x \leq 1.0$ the output of the Sobel and Laplacian filters are magnified by $\frac{1}{\Delta x}$ and $\frac{1}{\Delta x^2}$, respectively. Therefore, to avoid Euler integration from overshooting, we set $\Delta t = \min(1.0, \Delta x^2)$.

Figure 6 shows the output of all three NCA variants on two different textures for $\Delta x \in \{1.0, 0.5, 0.25\}$. The qualitative results in the figure show that *Noise-NCA* is able to generate the correct pattern across all values of Δx , while the baseline NCAs fail to generalize to different spatial resolutions. For a quantitative evaluation of the effect of Δx on the output quality, we use Δx values ranging from $[2^{-4}, 2^0]$, which results in grids with resolutions varying from 2048×2048 to 128×128 and test the models on 45 different textures. For a given value of Δx , let $S_T^{\Delta x}$ denote the output of NCA at time T given spatial discretization Δx and let \downarrow_{128} denote the bilinear interpolation operator for resizing to resolution 128×128 . As a measure of relative output quality, we evaluate the ratio of appearance losses

$$\frac{\mathcal{L}(S_T^{1.0})}{\mathcal{L}(\downarrow_{128} S_T^{\Delta x})}$$

for each NCA variant and show the results in Figure 7. The quantitative results show that *Noise-NCA* is better able to generalize to different spatial resolutions and maintains a higher quality compared to the baseline NCAs.

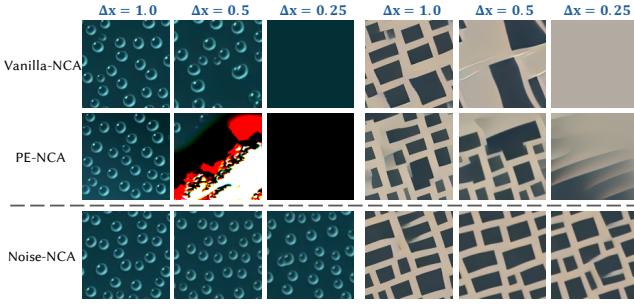


Figure 6: Output of NCA models for different resolutions with varying spatial discretization granularity Δx . As Δx decreases, the patterns created by *Vanilla-NCA* and *PE-NCA* start to deviate from the correct pattern, while *Noise-NCA* is able to maintain a consistent output.

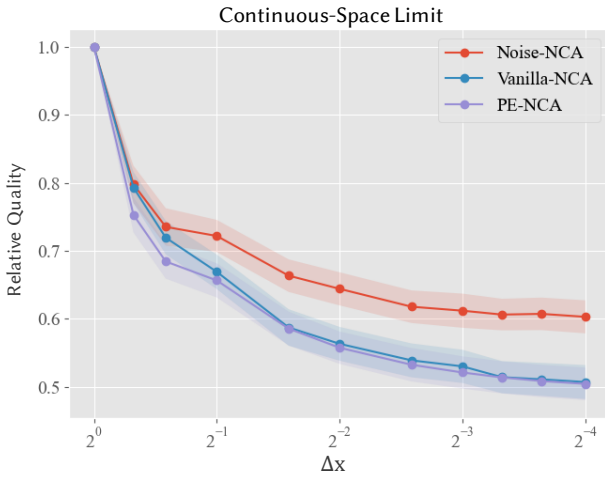


Figure 7: We simulate the NCA model on different spatial resolutions and evaluate the relative output quality for different values of Δx and show the results averaged over 45 textures. *Noise-NCA* shows improved generalization to different spatial resolutions compared to the baseline NCAs.

Our experiments demonstrate that *Vanilla-NCA* and *PE-NCA* overfit the spatial and temporal resolution used during training. This indicates that the dynamics learned by the baseline NCAs do not correspond to a continuous PDE, as they exhibit inconsistent behavior during training ($\Delta t, \Delta x, \Delta y = 1.0$) and inference ($\Delta t, \Delta x, \Delta y \rightarrow 0$). On the other hand, the dynamics learned by *Noise-NCA* behave much more consistently across different spatial and temporal resolutions. We also find that *Noise-NCA* achieves similar results if we modify the update rule at inference time by using alternative differential equation solvers such as the Runge-Kutta methods instead of the Euler method. These results show that our modifications to the NCA architecture improve the continuity of the dynamics learned by our *Noise-NCA* model and allow it to find an update rule that corresponds to an actual PDE.

Insights into the Overfitting Problem

In this section, we further investigate the NCA model and provide insights into the source of the overfitting. We also study the behavior of NCAs from a fixed point perspective to understand the output of overfitting NCA models at the limit $\Delta t \rightarrow 0$.

Source of Overfitting

Our experiments in the previous section demonstrate that *Vanilla-NCA* overfits to the timestep used during training, namely $\Delta t = 1.0$. We analyze this phenomenon and provide intuition that motivates and supports the design of *Noise-NCA*. We introduce two different scheduling policies $\Delta t_A(t), \Delta t_B(t)$ that will determine the timestep value Δt as a function of time t .

$$\Delta t_A(t) = \begin{cases} 1.0 & t \leq T_{crit} \\ 0.1 & t > T_{crit} \end{cases} \quad \Delta t_B(t) = \begin{cases} 0.1 & t \leq T_{crit} \\ 1.0 & t > T_{crit} \end{cases}$$

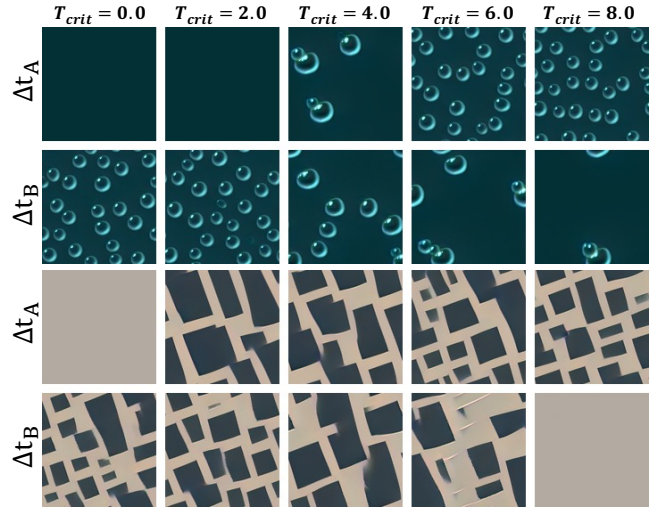


Figure 8: The output of *Vanilla-NCA* at $t = 300$ for different values of T_{crit} using two different schedulers $\Delta t_A(t), \Delta t_B(t)$.

T_{crit} in the above equations indicates the critical time at which the behavior of the scheduler will change. Given a scheduler, A or B , we use Euler integration to evaluate the output of *Vanilla-NCA* at $t = 300$ for different values of T_{crit} . Figure 8 shows the resulting output of *Vanilla-NCA* for five different values of T_{crit} . Notice that when $T_{crit} = 0.0$, *Vanilla-NCA* can successfully create the correct patterns using scheduler B as $\Delta t_B(t) = 1.0$, and fails to create the patterns using scheduler A since $\Delta t_A(t) = 0.1$. However, as T_{crit} increases, the output quality for scheduler A improves, while the opposite happens for scheduler B . Note that the time required for the patterns to be fully formed is around $t = 100$, and thus the values of T_{crit} used in our experiment are very small compared to pattern formation time. The results in Figure 8 suggest that *Vanilla-NCA* relies on the training timestep $\Delta t = 1.0$ when t is small

and the cell states are close to the seed state. We hypothesize that this overfitting occurs due to NCA’s reliance on stochastic updates to break the initial symmetry of the seed state. By replacing the zero seed state with uniform noise, *Noise-NCA* does not rely on stochastic updates to break the initial symmetry between cells and shows significantly improved generalization to unseen timesteps Δt , as shown in Figures 4, and 5.

Fixed Point Analysis

We find that at the continuous-time limit $\Delta t \rightarrow 0^+$, the behavior of the *Vanilla-NCA* model, either overfit or generalize, largely depends on the target texture. As shown in the second row of Figure 9, when Δt is small, for textures in Group B, the model is able to create the correct pattern, while for textures in Group A, it converges to a uniform solution that resembles the background color of the target pattern. We speculate that most target textures that have a clear background and foreground separation fall into Group A. In this section, we provide a fixed point analysis of the *Vanilla-NCA* model to better understand the overfitting problem and the nature of the uniform solution that *Vanilla-NCA* converges to. In this uniform solution, all cells converge to the same state and become stable. We refer to this state as a fixed point state $S_{fp} \in \mathbb{R}^C$ of the NCA. In the CA literature, this state S_{fp} is often referred to as a *Quiescent State* (Sayama, 2015). The property of the quiescent state is that if all neighbors of a cell, including the cell itself, are in the quiescent state, then the cell will remain in the quiescent state in the next iteration⁴. In the context of NCA, the quiescent state is a local fixed point of the NCA model.

If S_{fp} is a quiescent state of the NCA model, then the value of ΔS in Equation 2 should be close to zero. Let $Z_{fp} = [Z_{id}, Z_x, Z_y, Z_{lap}]$ be the perception vector of a cell in the quiescent state. Since all cells in the neighborhood are in the quiescent state, we can simplify the equation by using the fact that applying the Sobel and Laplacian filters to a constant neighborhood will give zero results. Therefore, $Z_x = Z_y = Z_{lap} = 0$ and $Z_{id} = S_{fp}$. Let $[W_1^{id}, W_1^x, W_1^y, W_1^{lap}]$ be a partitioning of the weight vector W_1 where each partition is a $D \times C$ matrix that operates on its corresponding part of the perception vector. To find a fixed point state of an NCA model we propose to solve the following optimization problem which minimizes the L_1 norm of the cell update ΔS :

$$S_{fp} = \arg \min_S \left\| W_2 (W_1^{id} S + b_1)_+ \right\|_1 \quad (8)$$

To find the fixed point state of an NCA, we numerically solve the optimization problem in Equation 8 using gradient descent. To visualize the obtained fixed point, we set the state of all cells to be equal to this fixed point state and show the results in the third row of Figure 9. These results

⁴For example in the Game of Life CA, dead states are quiescent states since a dead cell remains dead if all of its neighbors are dead.

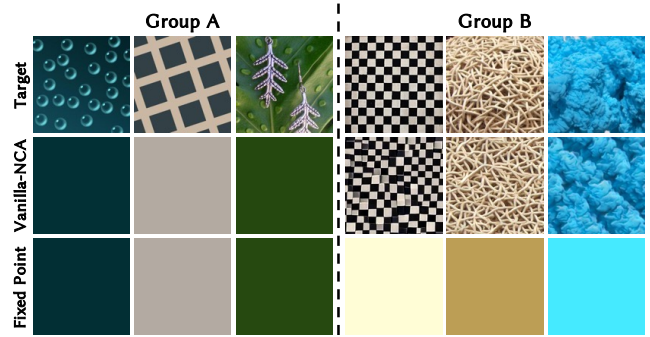


Figure 9: First row: Target texture, Second row: Output of *Vanilla-NCA* at $t = 300$ using $\Delta t = 0.001$. Third row: Fixed point state of the model obtained by numerically solving the optimization problem in Equation 8.

show that for textures in Group A, applying the NCA update rule with small Δt (illustrated in the second row of Figure 9) converges to the same state as the fixed point solution given by Equation 8. However, for textures in Group B, the model synthesizes the correct pattern using small values for Δt , showing that the NCA output does not converge to the fixed point solution. We hypothesize that this behavioral difference between Groups A and B is due to the stability of the fixed point state. In practice, the value of ΔS_{fp} is very close to but not exactly zero; therefore, the NCA model can escape from an unstable or saddle fixed point. We find that if we initialize the cell state with S_{fp} and apply the NCA update rule for a large number of steps, the NCA will escape the fixed point state and converge to the correct pattern for textures in Group B, while it will remain in the fixed point state for textures in Group A. This shows that the fixed point state is stable for textures in Group A and is a saddle point for textures in Group B. We speculate that for textures in Group A, when Δt is small, the stochastic update schema does not create enough variation between cells, which causes the NCA to converge to a fixed point with uniform state.

Scale of the Patterns

The cell size given by the values $\Delta x, \Delta y$ in Equation 5 controls the scale of the patterns. The smaller the cell size, the more cells (pixels) are required to create the pattern; therefore, the pattern becomes larger. In this section, we demonstrate three interesting ways to control and exploit the scale of the patterns at inference time.

Multiscale Patterns

By setting $\Delta x, \Delta y$ to be functions of the cell coordinate x, y , we can have local control over the scale of the synthesized patterns. In this example, we use a grid of size 256×1536 and vary the cell size as a function of the x coordinate, that is, $\Delta x = \Delta y = g(x)$. Figure 10 shows the results for 4 different textures. The target texture is shown on the left and the synthesized images demonstrating multiscale patterns are shown on the right. The function $g(x)$ is symmet-

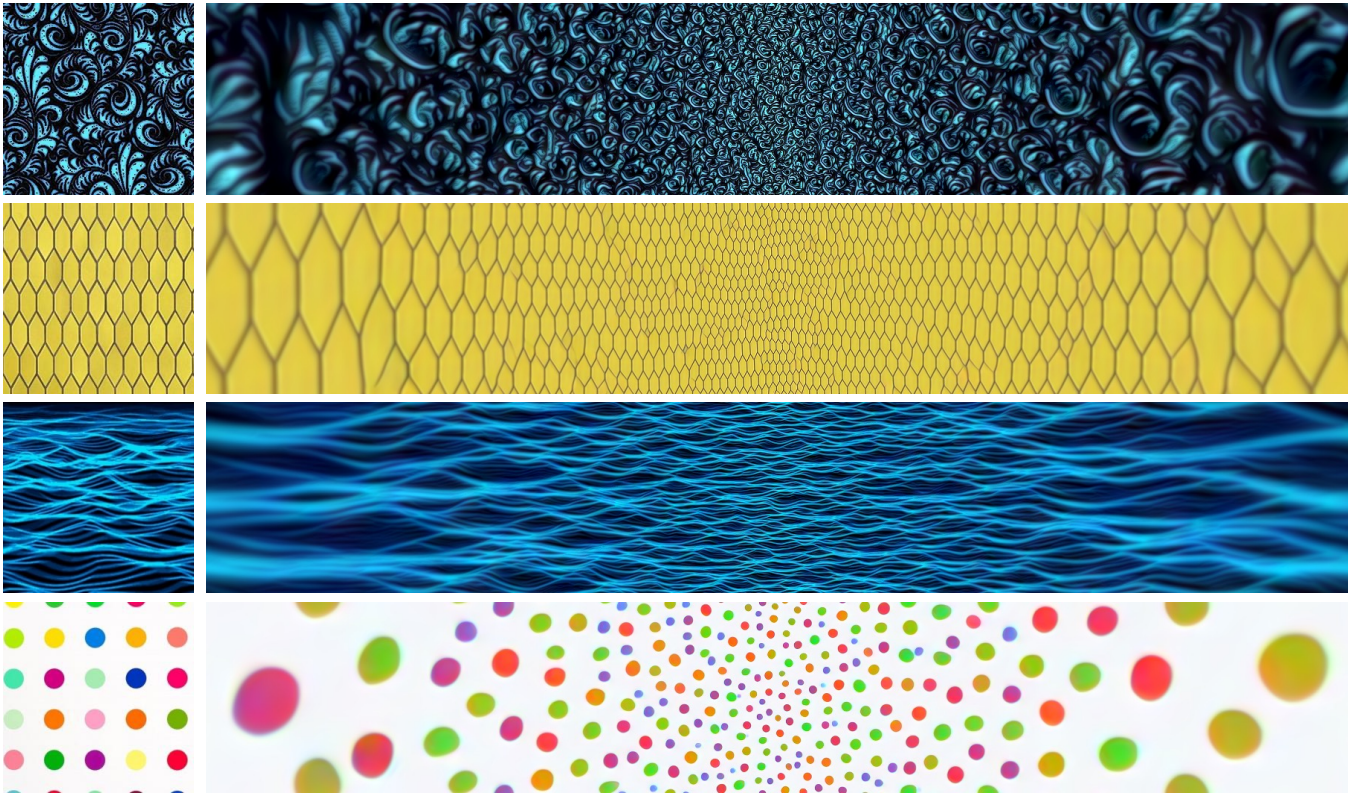


Figure 10: By varying the cell size $\Delta x, \Delta y$ as a function of the cell coordinate x, y , we can create multiscale patterns. The target texture is shown on the left and the synthesized images demonstrating multiscale patterns are shown on the right.

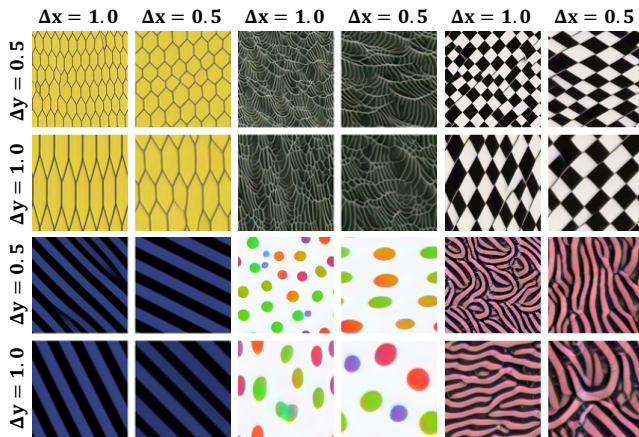


Figure 11: By using different values for $\Delta x, \Delta y$, *Noise-NCA* allows for anisotropic scaling. Decreasing $\Delta x, \Delta y$ stretches the patterns horizontally and vertically, respectively.

ric around the center of the image, increasing exponentially from $2^{-3.0}$ on the left border to $2^{0.5}$. This makes the patterns on the border to be roughly 11.0 times larger than the patterns in the center. Note how the scale of the patterns change smoothly and seamlessly across the image.

Anisotropic Scaling

Noise-NCA can create Anisotropically scaled patterns when $\Delta x \neq \Delta y$. In this example, we use two different values

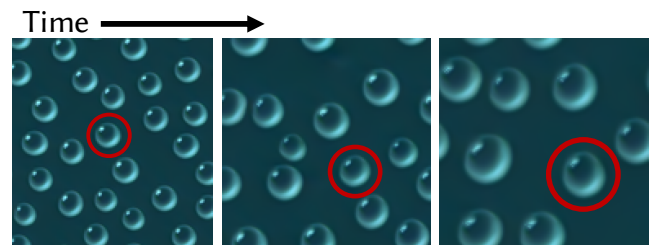


Figure 12: Varying the cell size $\Delta x, \Delta y$ over time t causes the patterns to grow or shrink. The red circle indicates a bubble that grows in size while remaining coherent.

for each dimension of the cell size $\Delta x, \Delta y \in \{1.0, 0.5\} \times \{1.0, 0.5\}$ and set the grid size to 128×128 regardless of the cell size. Figure 11 shows the anisotropic patterns for six different textures. Decreasing Δx is like stretching patterns horizontally, while decreasing Δy acts as a vertical stretch.

Time-Varying Scaling

Varying the cell size $\Delta x, \Delta y$ over time t causes the patterns to grow or shrink. We find that if the scale variation is smooth enough, the patterns remain coherent. For example, for the bubble pattern shown in Figure 12, when we decrease $\Delta x, \Delta y$ over time, some bubbles grow coherently in size without losing the whole bubble structure, as indicated by the red circle.

Conclusion

In this paper, we investigate whether NCA learns a continuous PDE that governs its dynamics or simply overfits the discretization used during training, by studying the NCA behavior at the continuous space-time limit. We show that existing NCA models struggle to generate correct textures when we change the space or time discretization, indicating overfitting. We analyze the source of the overfitting problem and propose *Noise-NCA*, an effective and easy-to-implement solution based on using random uniform noise as the seed. This change significantly improves NCA's ability to maintain consistent behavior across different discretization granularities and enables continuous control over the speed of the pattern formation and the scale of the synthesized patterns.

References

- Gardner, M. (1970). Mathematical games. *Scientific american*, 222(6):132–140.
- Mordvintsev, A. and Niklasson, E. (2021). μ nca: Texture generation with ultra-compact neural cellular automata. *arXiv preprint arXiv:2111.13545*.
- Mordvintsev, A., Randazzo, E., and Niklasson, E. (2021). Differentiable programming of reaction-diffusion patterns. In *Artificial Life Conference Proceedings 33*, volume 2021, page 28. MIT Press One Rogers Street, Cambridge, MA 02142-1209, USA journals-info
- Mordvintsev, A., Randazzo, E., Niklasson, E., and Levin, M. (2020). Growing neural cellular automata. *Distill*. <https://distill.pub/2020/growing-ca>.
- Niklasson, E., Mordvintsev, A., and Randazzo, E. (2021a). Asynchronicity in neural cellular automata. volume ALIFE 2021: The 2021 Conference on Artificial Life of *ALIFE 2023: Ghost in the Machine: Proceedings of the 2023 Artificial Life Conference*, page 116.
- Niklasson, E., Mordvintsev, A., Randazzo, E., and Levin, M. (2021b). Self-organising textures. *Distill*, 6(2):e00027–003.
- Otte, M., Delfosse, Q., Czech, J., and Kersting, K. (2021). Generative adversarial neural cellular automata. *arXiv preprint arXiv:2108.04328*.
- Pajouheshgar, E., Xu, Y., Mordvintsev, A., Niklasson, E., Zhang, T., and Süssstrunk, S. (2023a). Mesh neural cellular automata. *arXiv preprint arXiv:2311.02820*.
- Pajouheshgar, E., Xu, Y., Zhang, T., and Süssstrunk, S. (2023b). Dynca: Real-time dynamic texture synthesis using neural cellular automata. In *Proceedings of the IEEE/CVF Conference on Computer Vision and Pattern Recognition (CVPR)*, pages 20742–20751.
- Palm, R. B., González-Duque, M., Sudhakaran, S., and Risi, S. (2022). Variational neural cellular automata. *arXiv preprint arXiv:2201.12360*.
- Randazzo, E., Mordvintsev, A., Niklasson, E., Levin, M., and Greydanus, S. (2020). Self-classifying mnist digits. *Distill*. <https://distill.pub/2020/selforg/mnist>.
- Sandler, M., Zhmoginov, A., Luo, L., Mordvintsev, A., Randazzo, E., et al. (2020). Image segmentation via cellular automata. *arXiv preprint arXiv:2008.04965*.
- Sayama, H. (2015). *Introduction to the modeling and analysis of complex systems*. Open SUNY Textbooks.
- Simonyan, K. and Zisserman, A. (2015). Very deep convolutional networks for large-scale image recognition. In Bengio, Y. and LeCun, Y., editors, *3rd International Conference on Learning Representations, ICLR 2015, San Diego, CA, USA, May 7-9, 2015, Conference Track Proceedings*.
- Tesfaldet, M., Nowrouzezahrai, D., and Pal, C. (2022). Attention-based neural cellular automata. *arXiv preprint arXiv:2211.01233*.
- Turing, A. M. (1990). The chemical basis of morphogenesis. *Bulletin of Mathematical Biology*, 52(1):153–197.
- Von Neumann, J., Burks, A. W., et al. (1966). Theory of self-reproducing automata. *IEEE Transactions on Neural Networks*, 5(1):3–14.
- Wolfram, S. and Gad-el Hak, M. (2003). A new kind of science. *Appl. Mech. Rev.*, 56(2):B18–B19.